Creep mechanisms in glass-containing ceramics

D. Wilkinson, M. Chadwick

Creep mechanisms in glass-containing ceramics

D. S. Wilkinson and M. M. Chadwick

McMaster University, Hamilton, Ontario L8S 4L7, Canada

Résumé. — Le fluage des céramiques contenant une phase vitreuse est décrit en faisant une référence particulière aux résultats obtenus sur des nitrures de silicium frittés. Nous concluons qu'il y a deux mécanismes importants. Ce sont l'écoulement visqueux et le fluage par dissolution-précipitation. Les modèles pour ces processus sont passés en revue, et comparés à des résultats expérimentaux sur Si_3N_4. L'écoulement visqueux contrôle le comportement en fluage pour les faibles déformations à basse température ($\leqslant 1\ 250\ °C$). Nous avons des évidences de fluage par dissolution-précipitation à $1\ 325\ °C$.

Abstract. — The creep of glass-containing ceramics is outlined, with particular reference to data for sintered silicon nitride. We conclude that there are 2 important mechanisms. These are viscous flow, and dissolution-precipitation creep. The models for these processes are reviewed, and are compared with experimental data for Si_3N_4. At low strains and moderate temperatures ($\leqslant 1\ 250\ °C$), viscous flow controls the creep behaviour. However, we find evidence for dissolution-precipitation creep at $1\ 325\ °C$.

Introduction.

Many structural ceramic materials are difficult to sinter to full density. Silicon nitride is a good example. Diffusion is too slow for sintering to proceed at temperatures below that at which pure Si_3N_4 dissociates. It is therefore common to add oxide powders to aid in sintering. These produce a liquid phase during sintering which greatly enhances mass transport. In the case of Si_3N_4, the oxides most commonly used are Y_2O_3 and Al_2O_3, typically several weight percent of each. The liquid also contains SiO_2 which is always present on the surface of Si_3N_4 powders. In the case of Si_3N_4, the liquid has a secondary function-namely to enhance the transformation of α-Si_3N_4 to the β phase. Following liquid-phase sintering, the liquid either solidifies into one or more crystalline phases, or forms a glass (or some combination of these).

In this paper, we discuss the creep behaviour of ceramics which contain an intergranular glass phase following sintering. A model for creep by viscous flow is presented, and discussed in relation to creep studies on sintered Si_3N_4.

Creep behaviour of sintered silicon nitride.

A detailed description of the material used in this study, and of the experimental methods
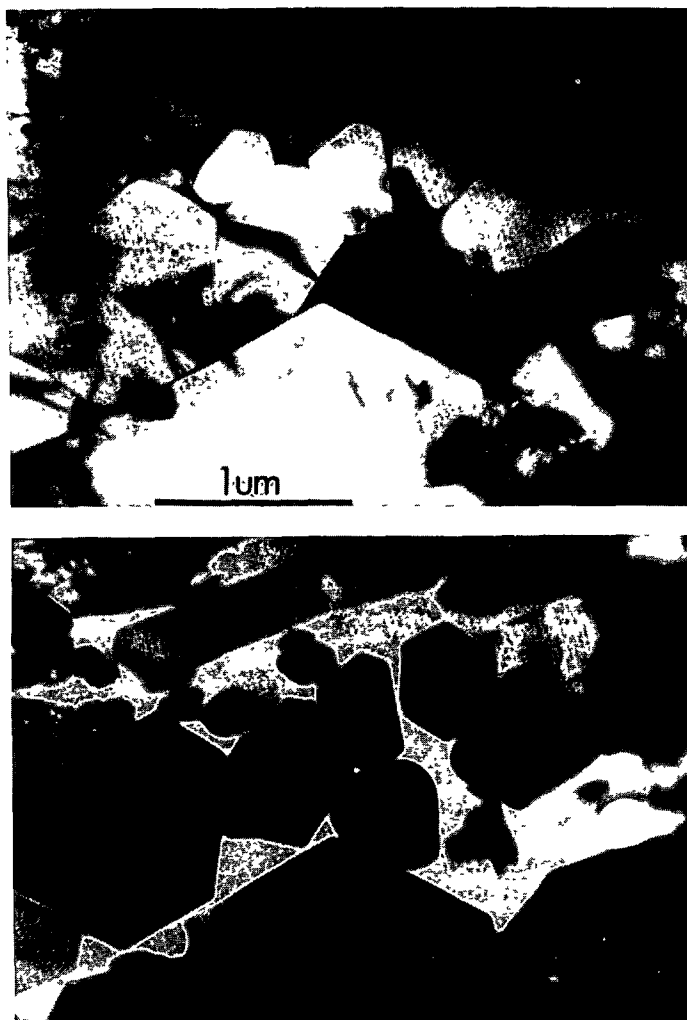
Fig. 1. — Bright field/dark field TEM micrographs of the as-received microstructure, showing the amorphous grain boundary phase.

employed, is given elsewhere [1, 2]. The material in a commercial Si_3N_4, Kyocera SN220, containing Y_2O_3 and Al_2O_3. By means of neutron activation analysis the additive amounts have been estimated at 4.2 wt% Y_2O_3 and 3.8 wt% Al_2O_3. The microstructure consists of β-Si_3N_4 grains, ranging in size from 0.25 to 1.5 μm, with some elongated grains 3 to 8 μm in length (see Fig. 1). In addition, the material contains a Y_2O_3-Al_2O_3-SiO_2 glass. This appears both as thin layers between grain boundaries, and as pockets interspersed amongst the Si_3N_4 grains. Upon annealing, in the temperature range 1 200-1 250 °C, this glass partially crystallizes. The extent of crystallization and the crystalline products formed depend on position within the sample, as indicated in figure 2. The dominant crystalline phases in the interior are $Y_2Si_2O_7$ and YAG ($Al_5Y_3O_{12}$). These phases are also found near the surface of samples annealed in an inert atmosphere. However, when the samples are annealed in air, devitrification is accompanied by oxidation and YAG is no longer found. Instead, mullite ($Al_6Si_2O_{13}$) is seen along with $Y_2Si_2O_7$. Figure 2 also gives the results of an extensive analysis

Air (Centre) and
Inert Anneal
1250°C

20 ± 3 w/o $Y_2Si_2O_7$
19 ± 4 w/o $Y_3Al_5O_{12}$
61 ± 7 w/o residual glass

Air Anneal (Surface)
1250°C

50 ± 8 w/o $Y_2Si_2O_7$
22 ± 5 w/o $Al_6Si_2O_{13}$
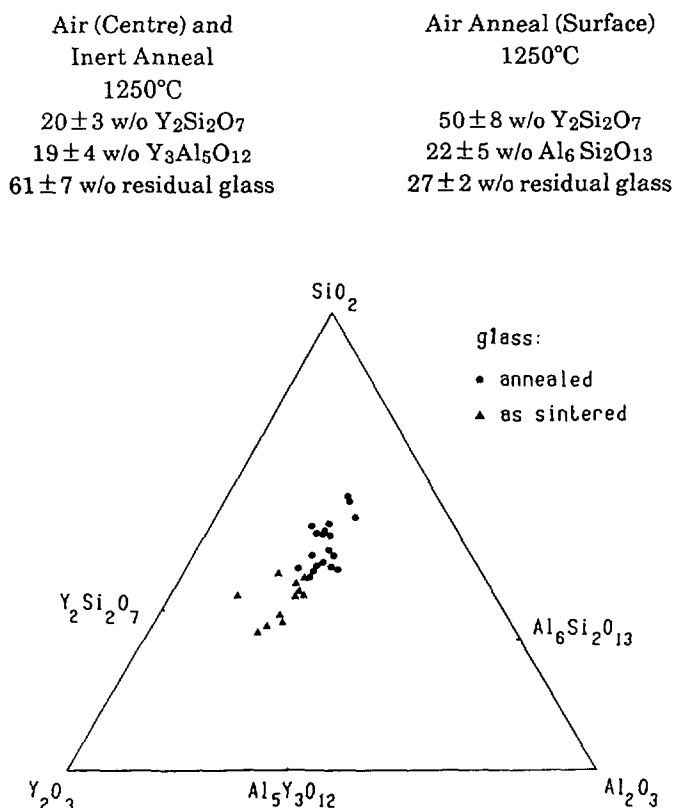27 ± 2 w/o residual glass

Fig. 2. — The composition of grain boundary glass, both before and after annealing are indicated on this Y_2O_3-Al_2O_3-SiO_2 ternary diagram, along with the phases that precipitate from the glass.

of glass composition, before and after annealing, using electron energy loss spectroscopy (EELS) of thin foils in the electron microscope.

The application of EELS to the analysis of amorphous regions offers some advantage over energy dispersive X-ray spectroscopy (EDS). However, a new methodology needs to be developed in order to obtain quantitative analyses to within 5 % accuracy. The details of such a methodology, along with the condition used for the current analysis, are published elsewhere [11]. Figure 2 shows the glass composition before and after annealing. Two points are noteworthy. First, there is a systematic shift in the glass composition to higher SiO_2 contents, with a new stable composition developing within 200 hours at 1 250 °C. Second, the glass composition after annealing is independent of the crystalline phase formed. An elemental mass balance has been used to assess the degree of recrystallization. This indicates that within the bulk material, about 60 % of the glass remains in the vitreous state. The Si_3N_4 grains do not appear to participate in this process (i.e. nitrogen is not dissolved into the glass up to the detectability limit of about 5 %). The crystalline phases are difficult to nucleate and extend around several Si_3N_4 grains (see Fig. 3). As noted above, the nature of the crystalline products is different near the surface of the specimens. Moreover, the extent of crystallization is considerably greater. However, since creep sample surfaces were refinished following annealing, this difference in crystallization behaviour near the surfaces does not affect the creep results reported below.

Four-point bend creep studies of this material, both in the as-sintered condition and

Fig. 3. — A bright field-dark field pair of Kyocera SN 220 following annealing. A $Y_2Si_2O_7$ particle has nucleated and grown around several Si_3N_4 grains.

following annealing, have been performed. The creep appears at first sight to be quite normal (Fig. 4). However, careful analysis of the creep strain rate $\dot{\varepsilon}$ as a function of time or strain (Fig. 5) shows a steady-state region at low strains (< 0.3 % at 1 200 °C) followed by a region of continuously decreasing strain rate. The steady-state region exhibits power-law behaviour ($\dot{\varepsilon} \sim \sigma^n$) with an exponent n, of 4. The critical strain at which the strain rate begins to decrease ε_c, also increases with stress, although weakly. Prior annealing does not significantly alter the steady-state strain rate. It does, however, reduce ε_c slightly.

Testing has also been performed in compression. The results are broadly similar. However, the region of decreasing strain rate occurs at much lower strains than in bending. Consequently, steady-state behaviour is not generally observed.
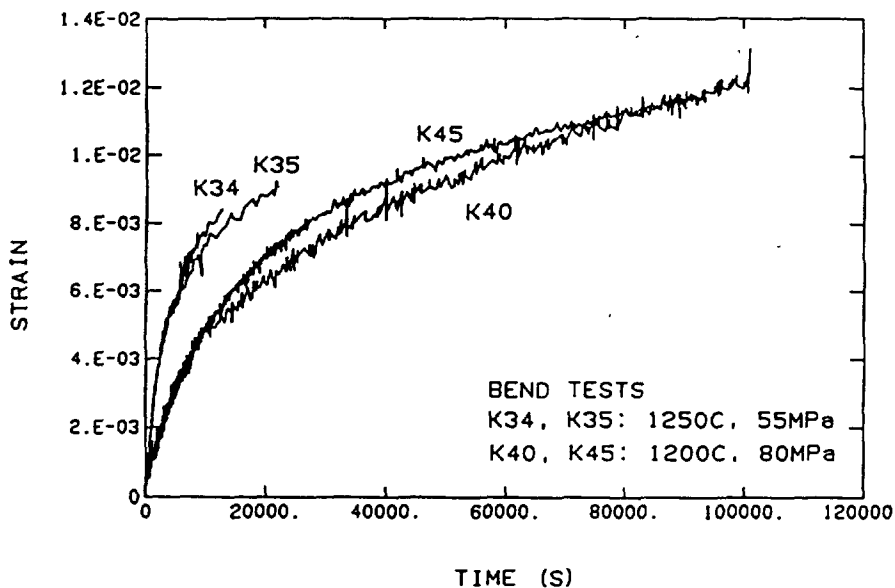

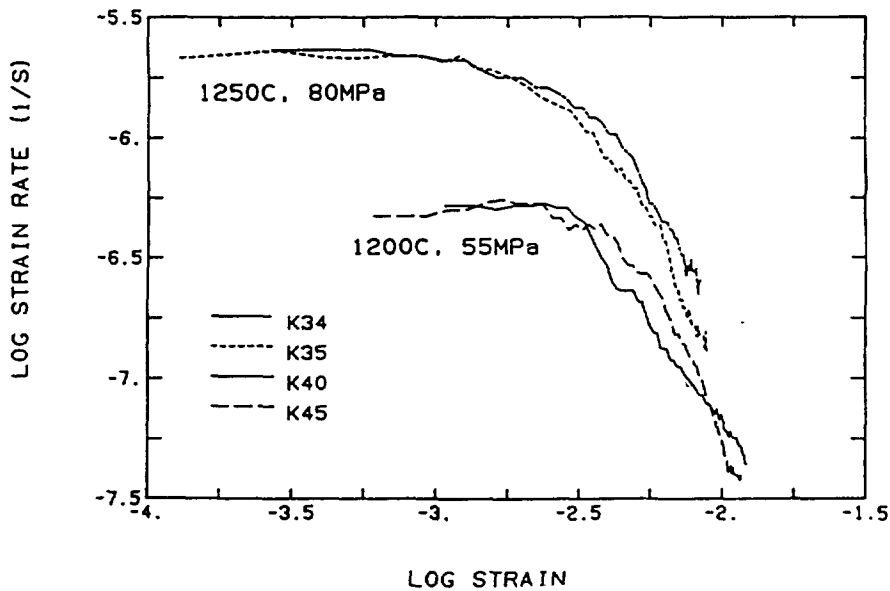Fig. 4. — A set of typical creep curves for SN 220.

Fig. 5. — Strain rate-strain plots for the same data as in figure 3, showing a typical plateau region followed by a rapid decrease in strain rate.

The effect of creep on devitrification has also been studied using the technique described above. Within the experimental accuracy of the technique, we find no difference in the glass composition in tension or compression, or as compared with samples annealed in the absence of stress.

Creep mechanisms.

Several models have been proposed to explain the creep of glass-containing ceramics, and these will be briefly reviewed here.

The glass acts, first of all, as a fast diffusion path, in which material is dissolved at boundaries of low or negative stress, and redeposits at boundaries of high stress. Thus, a modified version of the Coble creep equation can be developed [3] :

$$\dot{\varepsilon} = \alpha \, \frac{C_g \, D_g}{kT} \frac{H}{L^3} \sigma \tag{1}$$

where C_g is the solid solubility of the crystalline phase in the glass and D_g the diffusion coefficient in the glass, H is the glass layer thickness and L the grain size. Raj and Chyung [4] later noted that this mechanism could be controlled, not by the diffusion kinetics, which may be quite rapid, but by the kinetics of dissolution. This leads to a modified equation for creep :

$$\dot{\varepsilon} = \frac{K\Omega}{kTL} \sigma$$

where K is the kinetic constant for dissolution.

An alternative mechanism involving dissolution has been proposed by Pharr and Ashby [5]. Here it is supposed that dislocation plasticity occurs at points of contact between grains,

alternating with dissolution of the interfaces thus produced by the glassy phase. This leads to an equation for creep of the form

$$\dot{\varepsilon} \sim \frac{D_g\, C_g\, Y_s\, \Omega}{kTL^3}\, f(\sigma)$$

where Y_s is the solid-glass interfacial energy and $f(\sigma)$ is a complex function of the stress state.

Another possible creep mechanism involves viscous flow of the glass phase, as illustrated in figure 6. There have been several models developed for this process. Some of these, for example, that by Pharr and Ashby [5], treat only the shear of a viscous fluid. This ignores the constraint imposed by the impingent of adjacent grains. Thus a realistic model must consider the squeezing of liquid from between the grains, driven by a pressure gradient along the interfaces. Such a model, for a linear viscous fluid, has been developed by Drucker [6] and

$$2\dot{H} = \left(\frac{H}{L}\right)^3 \frac{F}{\eta} \qquad\qquad 2\dot{H} = \left(\frac{H}{L}\right)^3 \frac{(F + 2LP)}{\eta}$$
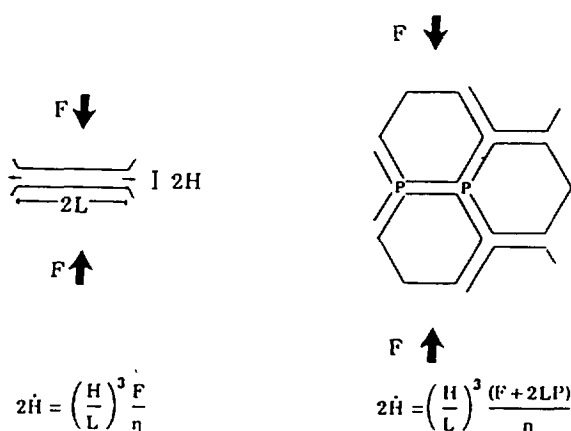
Fig. 6. — A schematic illustration of creep controlled by viscous flow.

extended to include the strain dependence of flow by Dryden *et al.* [7]. This leads to a creep rate of the form :

$$\dot{\varepsilon} = \frac{3}{8} \frac{f^3\, \sigma S(\varepsilon_N)}{\eta}$$

where η is the glass viscosity, f is the normalized glass layer thickness ($f = 2H/\sqrt{3}\,L$), and S is a function of the normalized strain $\varepsilon_N (= \varepsilon/f)$:

$$S(\varepsilon_N) = \frac{3(1 - \varepsilon_N)^3\, (1 + 2\,\varepsilon_N)^3}{(1 + 2\,\varepsilon_N)^3 + 2(1 + \varepsilon_N)^3}.$$

More recently this model has been further extended to consider the case of a non-linear viscous glass with a constitutive law of the form $\dot{Y} = \phi\tau^n$, where $\dot{Y}$ and τ are the shear strain rate and stress respectively, while ϕ and n are material constants [8]. In this case the creep rate has the form

$$\dot{\varepsilon} = C\phi R(\varepsilon_N)|\sigma|^n$$

where

$$C = \frac{3^{(n+1)/2}}{2^{n+1}(n+2)} \left[\frac{2n+1}{2n} \right]^n f^{n+2} \operatorname{sgn}(\sigma)$$

and

$$R(\varepsilon_N) = 3^n \frac{(1 + 2\varepsilon_N)^{n+2} (1 - \varepsilon_N)^{n+2}}{[(1 + 2\varepsilon_N)^{(n+2)/n} + 2^{1/n}(1 - \varepsilon_N)^{(n+2)/n}]^n}.$$

The strain rate dependence function $R(\varepsilon_N)$, is plotted as a function of strain in figure 7, assuming a creep exponent $n = 4$, and using the same log-log scale used to plot the creep data (see Fig. 5). It shows a region of constant strain rate, followed by a decrease in strain rate above a critical strain. The maximum strain which can be achieved by this mechanism is greater in tension than in compression, by a factor of two.
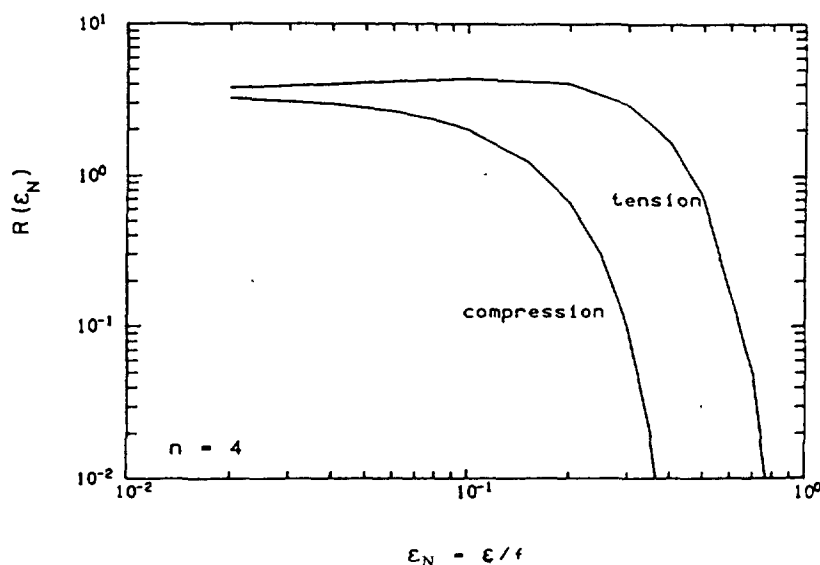

Fig. 7. — The strain dependent function $R(\varepsilon_N)$ is plotted as a function of normalized strain ε_N for tension and compression.

Discussion.

The creep of sintered silicon nitride at 1 200-1 250 °C exhibits two distinct regimes. Below a critical strain, the strain rate is constant. Above this strain, it starts to decrease rapidly. This behaviour cannot be explained by models for flow based on diffusion through the glass, since these predict a steady-state over a wide range of strain. Moreover, there is no evidence, based on TEM observations, of any dislocation activity of the type required by the Pharr and Ashby model for dissolution enhanced plasticity. The data therefore suggests that viscous flow is the most likely mechanism for creep in this material. The models for this process [7, 8] do predict a strain-dependent creep rate (see Fig. 7) which is consistent with that observed (Fig. 5). The drop in strain rate predicted by the model has been fit to the data using the glass viscosity parameter ϕ and the glass layer thickness H, as the adjustable parameters. The viscosity parameter fixes the value of the plateau strain rate, while H fixes the strain at which the creep
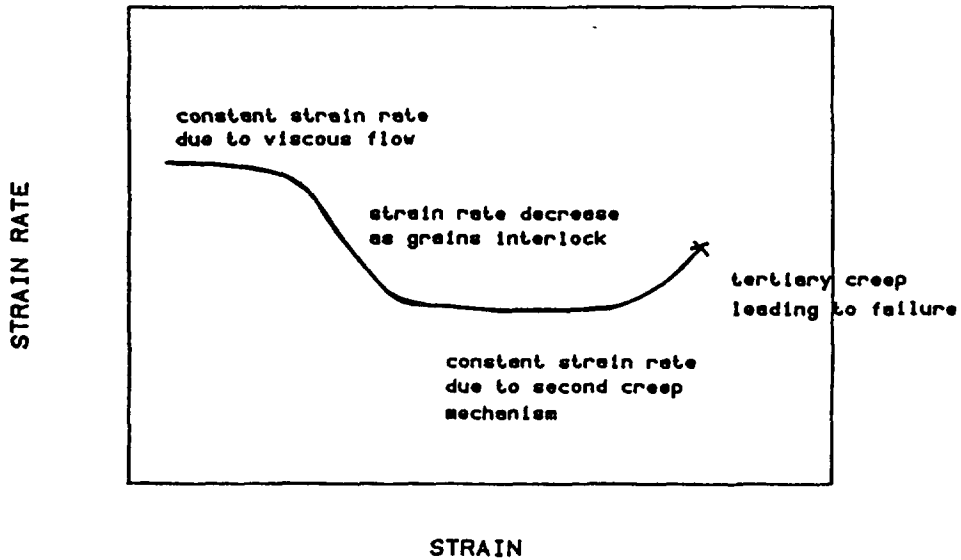
Fig. 8. — A schematic strain rate-strain curve indicating the transition from viscous flow at low strains to a different mechanism (e.g. dissolution-precipitation creep) at higher strains.
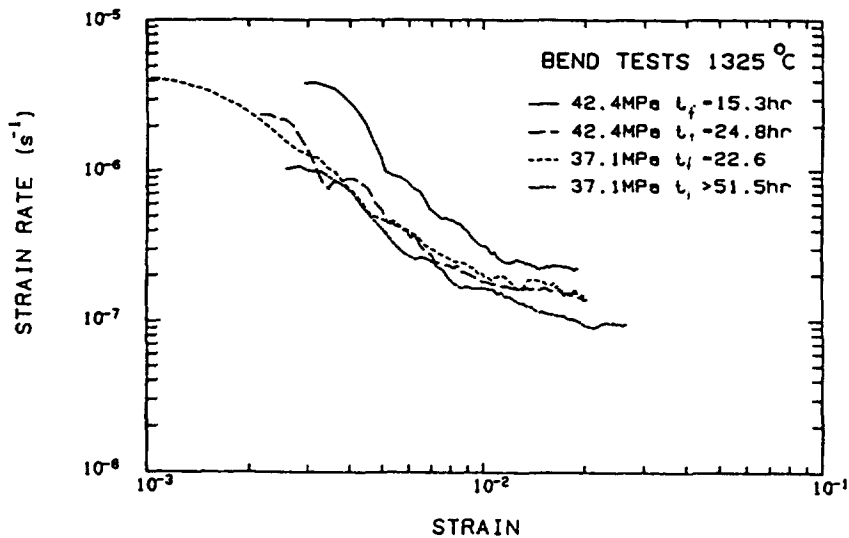

Fig. 9. — The creep behaviour of SN 220 at 1 325 °C, indicating a transition to a second creep mechanism.

rate drops. The shape of the $\dot{\varepsilon} - \varepsilon$ curve is predicted very well in this way. Moreover, the value of H used is in the range 14-20 nm. This is in reasonable agreement with the observations of Clarke [9] of glass thickness between 2 and 10 nm in MgO doped Si_3N_4 which had been quenched from 1 450 °C. We therefore conclude that viscous flow controlled creep is responsible for the creep behaviour of this material in the range 1 200 to 1 250 °C.

The question remains however, as to the general applicability of this conclusion. It seems likely for example, that under different conditions the process of dissolution-precipitation creep will be important. We therefore postulate a scenario as outlined in figure 8. In most glass-containing ceramics, at temperatures required for creep, the glass will have a low or modest viscosity and can be expected to flow. For modest viscosities, the viscous flow process will be expected to dominate at low strain and for measurable times. Following this, the strain rate will decrease. If the rate of dissolution-precipitation creep is sufficient, a new steady-state will then be established. We have studied this possibility in Kyocera SN220 at 1 325 °C (Fig. 9). At this higher temperature, the viscous flow regime is over very quickly. There is clear evidence at larger strains of the approach to a new steady-state, although fracture generally intervenes.

If the viscosity of the glass is very low, then the viscous flow regime will be very short. Indeed, it will be completed during the period of specimen loading. Thus the viscous flow strain will become part of the initial loading strain. This is the case for 2-phase alloys above the melting temperature of one of the phases (see for example, the work of Vaandrager and Pharr [10] on copper containing liquid bismuth).

Conclusions.

The creep of glass containing ceramics occurs by a combination of viscous flow and dissolution-precipitation creep. Viscous flow tends to dominate at low strains but is limited to a strain of order H/L, where H is the thickness of the intergranular glass, and L is the grain size. Dissolution-precipitation creep is observed at higher strains, but only if the strain rate due to this mechanism is high enough. Thus, for the material studied here, at temperatures up to 1 250 °C, only viscous flow is observed. Both mechanisms are apparent, however, at 1 325 °C.

References

[1] CHADWICK M. M., Ph. D. Thesis, McMaster University (1990).
[2] CHADWICK M. M. and WILKINSON D. S., to be published (1991).
[3] STOCKER R. L. and ASHBY M. F., *Rev. Geophys. Space Phys.* 11 (1983) 391.
[4] RAJ R. and CHYUNG C. K., *Acta Metall.* 29 (1981) 159.
[5] PHARR G. M. and ASHBY M. F., *Acta Metall.* 31 (1983) 129.
[6] DRUCKER D. C., in High Strength Materials, Ed. V. F. Zachay (Wiley Press) 1964, p. 795.
[7] DRYDEN J. R., KUCEROVSKY D., WILKINSON D. S. and WATT D. F., *Acta Metall.* 37 (1989) 2007.
[8] WILKINSON D. S., CHADWICK M. M. and DRYDEN J. R., to be published (1991).
[9] CLARKE D. R., *J. Am. Ceram. Soc.* 72 (1989) 1604.
[10] VAANDRAGER B. L. and PHARR G. M., *Acta Metall.* 37 (1989) 1057.
[11] CHADWICK M. M. and MALIS T. F., *Ultramicroscopy* 31 (1989) 205.